

AD-A152 762

THE TEMPERATURE DEPENDENCE OF DIFFRACTED BEAM  
INTENSITIES IN ATOM-SURFACE. (U) CALIFORNIA UNIV SANTA  
BARBARA DEPT OF CHEMISTRY B JACKSON ET AL. MAR 85

1/1

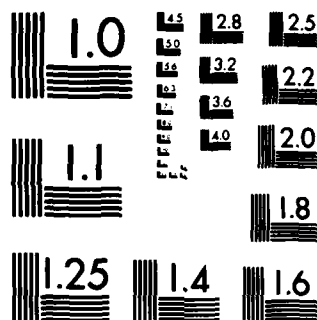
UNCLASSIFIED

TR-16 N00014-81-K-0598

F/G 20/8

NL

								END				
								FILED				
								DIR				



MICROCOPY RESOLUTION TEST CHART  
NATIONAL BUREAU OF STANDARDS-1963-A

unclassified/unlimited

SECURITY CLASSIFICATION OF THIS PAGE (When Data Entered)

2

AD-A152 762

REPORT DOCUMENTATION PAGE		READ INSTRUCTIONS BEFORE COMPLETING FORM
1. REPORT NUMBER 16	2. GOVT ACCESSION NO.	3. RECIPIENT'S CATALOG NUMBER
4. TITLE (and Subtitle) THE TEMPERATURE DEPENDENCE OF DIFFRACTED BEAM INTENSITIES IN ATOM-SURFACE SCATTERING		5. TYPE OF REPORT & PERIOD COVERED Annual Tech Report
		6. PERFORMING ORG. REPORT NUMBER
7. AUTHOR(s) Bret Jackson and <u>Horia Metiu</u>		8. CONTRACT OR GRANT NUMBER(s) N00014-81-K-0598
9. PERFORMING ORGANIZATION NAME AND ADDRESS University of California Department of Chemistry Santa Barbara, CA 93106		10. PROGRAM ELEMENT, PROJECT, TASK AREA & WORK UNIT NUMBERS NR 056-766/4-21-81 (472)
11. CONTROLLING OFFICE NAME AND ADDRESS Office of Naval Research Department of the Navy, Code: 612A:DKB Arlington, VA 22217		12. REPORT DATE March 1985
		13. NUMBER OF PAGES 32
14. MONITORING AGENCY NAME & ADDRESS (if different from Controlling Office) Office of Naval Research Detachment Pasadena 1030 East Green Street Pasadena, CA 91105		15. SECURITY CLASS. (of this report) unclassified/unlimited
		15a. DECLASSIFICATION/DOWNGRADING SCHEDULE
16. DISTRIBUTION STATEMENT (of this Report)  This documentation has been approved for public release and sale; its distribution is unlimited.		
17. DISTRIBUTION STATEMENT (of the abstract entered in Block 20, if different from Report)		
18. SUPPLEMENTARY NOTES Submitted to the Journal of Chemical Physics		
19. KEY WORDS (Continue on reverse side if necessary and identify by block number)		
20. ABSTRACT (Continue on reverse side if necessary and identify by block number) We develop a new method for the calculation of the atom scattering analog of the Debye-Waller factor. Unlike X-ray and neutron scattering the properties of an atom scattered by a solid surface cannot be computed by perturbation theory, therefore the simple Debye-Waller theory cannot be applied. Never- theless the Debye-Waller phenomenon has a close analog: the elastic intensity is depressed due to the uncorrelated part of the thermal motion of the lattice atoms. To compute this effect we develop a time dependent scattering theory in which the quantum properties of the scattered atom are described by		

DTIC  
JAN 1985  
E

DTIC FILE COPY

DD FORM 1 JAN 73 1473

EDITION OF 1 NOV 65 IS OBSOLETE  
S/N 0102 LF 014-6601

Unclassified/unlimited

SECURITY CLASSIFICATION OF THIS PAGE (When Data Entered)

85

Propagating coherently an ensemble of wave packets and lattice motion is simulated by a classical Langevin equation. Applications are made to He and Ne scattering from a surface whose lattice dynamics mimics that of Pt(111) but whose corrugation was slightly increased to enrich the diffraction structure.

OFFICE OF NAVAL RESEARCH

Contract N00014-81-K-0598

Task No. NR 056-766/4-21-81 (472)

Technical Report No. 16

THE TEMPERATURE DEPENDENCE OF DIFFRACTED BEAM  
INTENSITIES IN ATOM-SURFACE SCATTERING

by

B. Jackson and H. Metiu

J. CHEM. PHYS., submitted (1985)

University of California  
Department of Chemistry  
Santa Barbara, CA 93106

Accession For	
NTIS GRA&I	<input checked="" type="checkbox"/>
DTIC TAB	<input type="checkbox"/>
Unannounced	<input type="checkbox"/>
Justification	
By _____	
Distribution/	
Availability Codes	
Dist	Avail and/or Special
A-1	



Reproduction in whole or in part is permitted for  
any purpose of the United States Government.

This document has been approved for public release  
and sale; its distribution is unlimited.

The Temperature Dependence of Diffracted Beam Intensities  
in Atom-Surface Scattering.

Bret Jackson and Horia Metiu

Department of Chemistry  
University of California  
Santa Barbara, California 93106

## ABSTRACT

↙ We develop a new method for the calculation of the atom scattering analog of the Debye-Waller factor. Unlike X-ray and neutron scattering the properties of an atom scattered by a solid surface cannot be computed by perturbation theory, therefore the simple Debye-Waller theory cannot be applied. Nevertheless the Debye-Waller phenomenon has a close analog: the elastic intensity is depressed due to the uncorrelated part of the thermal motion of the lattice atoms. To compute this effect we develop a time dependent scattering theory in which the quantum properties of the scattered atom are described by propagating coherently an ensemble of wave packets and lattice motion is simulated by a classical Langevin equation. Applications are made to He and Ne scattering from a surface whose lattice dynamics mimics that of Pt(111) but whose corrugation was slightly increased to enrich the diffraction structure. ^

## I. Introduction

The diffraction of atoms by solids<sup>1</sup> has many useful applications in surface science, particularly as a probe of both surface structure and dynamics. The shapes and intensities of the diffraction peaks are very sensitive to the thermal motion of the surface atoms. In this paper we present a theory for the effect of this motion on the elastic diffraction peak probabilities; that is, for the atom scattering analog of the Debye-Waller factor appearing in x-ray and neutron scattering. Prior work has discussed<sup>2</sup> such effects by taking over, with slight modifications the Debye-Waller formula from neutron scattering theory. Weinberg<sup>2f</sup>, Hoinkes, Nahr, and Wilsch<sup>3</sup>, and others<sup>2</sup> used the resulting equation to extract values for the surface Debye temperature of the lattice atoms and the results obtained are reasonable. So, while this procedure is not terribly misleading it is suspect, from a theoretical point of view, on several counts. The derivation of the Debye-Waller factor in neutron scattering<sup>4</sup> relies heavily on the fact that the neutron-nucleus interaction can be described by the Fermi pseudopotential.<sup>5</sup> As a result the collision of the neutron with a given nucleus can be calculated by using the Golden Rule and the potential has zero range. Furthermore, the neutron-lattice interaction is so weak that we can assume that the neutrons passing through the sample have been scattered once (i.e. by one nucleus) or not at all. Clearly none of these conditions hold for atom scattering. A more detailed analysis of the difference between atom and neutron scattering and of the reasons why such differences affect the Debye-Waller factor can be found in Appendix 1.

The application of the usual<sup>6</sup> coupled channels method to collisions with a surface undergoing thermal motion seems impractical unless the phonon-particle interactions are treated within perturbation theory (the distorted wave approxima-



tion).<sup>17</sup> It is not clear, however, whether perturbation theory is adequate for this situation. One would therefore like to have a non-perturbative approach to this problem. One possibility is to treat the motion of the lattice classically and the scatterer by quantum theory. In general such an approach has difficulties since a replacement of some of the quantum variables by their classical trajectories leads to ambiguities in defining the proper classical (Newton) equations<sup>8</sup>; the theory does not (in the simplest cases) provide a feedback mechanism by which the classical degrees of freedom are "informed" that they have to change their energy when the quantum ones are changing theirs.

One way of avoiding such difficulties is to treat the quantum degrees of freedom by a method which is very compatible with classical mechanics. The possibility which we pursue here is the wave packet method developed by Heller and his coworkers<sup>9</sup> and applied to diffraction by a static lattice by Droschlagen and Heller (DH).<sup>10</sup> The method consists of writing the incident planar wave as a sum of Gaussian wave packets, propagating them independently by using the time dependent Schroedinger equation and constructing the scattered wave function by adding coherently the scattered packets. The theory reduces the wave packet propagation to the calculation of the time evolution of the position of the center of the wave packet, its mean momentum, and its width and phase. The center of the packet and the momentum evolve according to the classical equations of motion, the phase at the end of the trajectory is the classical action and the width satisfies a first order differential equation. All these quantities depend on the instantaneous position of the lattice atoms through the classical atom-lattice interaction. We propagate the lattice atom positions by using the Adelman-Doll-Tully<sup>12</sup> method (ADT) which provides a Langevin equation for the motion of the surface atoms involved in the collision with the probe atom. As a result of combining the Langevin equation for the surface atoms with the wave packet description of the

incident particle the motion of the packet is modified as follows: the position  $r_t$  and the momentum  $p_t$  of its center are now stochastic variables evolving according to a classical Langevin equation; the phase which depends on  $r_t$  and  $p_t$  is also randomized, thus creating a dephasing which leads to a decrease in the diffraction peaks intensity and an increase in the background scattering. The width-which provides a space dependent phase and an amplitude- also becomes a random variable.

## II. THE METHOD

Since we plan to treat the lattice motion classically we start with the customary classical trajectory approximation method (CTA). If the Hamiltonian depends on two sets of variables  $x$  and  $y$  and we want to treat  $y$  classically then we use the "reduced" Hamiltonian

$$H(x, y(t)) = -(\hbar^2/2m) \nabla_x^2 + V(x, y(t)) \quad (II.1)$$

The kinetic energy operator  $-(\hbar^2/2m)\nabla_y^2$  is removed from the Hamiltonian since this quantity is included in the classical equation of motion for  $y(t)$ . The potential energy and the wave function  $\psi(x; y(t))$  depends on the classical variable  $y(t)$  parametrically. In the present case the quantum variable  $x$  is the atom position  $\vec{r}$  and the group of classical variables  $y(t)$  is the set  $\vec{R}_i(t)$  of lattice atom positions.

Following DH we write the time dependent wave function  $\psi(\vec{r}, t)$  of the incident atom in the form

$$\psi(\vec{r}; t) = \sum_{\alpha} G_{\alpha}(\vec{r}; \{\lambda_{\alpha}(t)\}) \quad (II.2)$$

where  $G_{\alpha}$  is a Gaussian wave packet (GWP) given by

$$G_{\alpha}(\vec{r}, \{\lambda_{\alpha}(t)\}) = \exp\left\{\frac{i}{\hbar}[(\vec{r} - \vec{r}_{\alpha}(t)) \cdot \vec{A}_{\alpha}(t) \cdot (\vec{r} - \vec{r}_{\alpha}(t)) - \vec{p}_{\alpha}(t) \cdot (\vec{r} - \vec{r}_{\alpha}(t)) + \gamma_{\alpha}(t)]\right\} \quad (II.3)$$

The set  $\{\lambda_{\alpha}(t)\}$  is a symbolic notation for the time dependent parameters  $\vec{A}_{\alpha}$ ,  $\vec{r}_{\alpha}(t)$ ,  $\vec{p}_{\alpha}(t)$  and  $\gamma_{\alpha}(t)$ . The parameters  $\vec{r}_{\alpha}(t)$  and  $\vec{p}_{\alpha}(t)$  are the expectation values of the position and momentum of the packet

$$\begin{pmatrix} \vec{r}_\alpha(t) \\ \vec{p}_\alpha(t) \end{pmatrix} = \int d\vec{r} G_\alpha(\vec{r}; \{\lambda_\alpha(t)\})^* \begin{pmatrix} \vec{r} \\ -i\hbar \frac{\partial}{\partial \vec{r}} \end{pmatrix} G_\alpha(\vec{r}; \{\lambda_\alpha(t)\}) \quad (II.4)$$

The complex quantity  $\gamma_\alpha(t)$  generates the phase  $\text{Re} \gamma_\alpha(t)/\hbar$  and the amplitude  $\exp\{-\text{Im} \gamma(t)/\hbar\}$  of the packet. The three dimensional square matrix  $\vec{A}_\alpha(t)$  controls the width of the packet (through its imaginary part), generates a space dependent phase (through its real part) and couples the variables  $x, y, z$  (in the interaction region) through its off-diagonal elements.

The time evolution of the wave function  $\psi(\vec{r}; t)$  is obtained by what we call the simplest Heller method (SHM). This forces the parameters  $\lambda_\alpha(t)$  to vary in time so that each Gaussian satisfies the time dependent Schrodinger equation

$$\left[ -(\hbar^2/2m) \nabla_{\vec{r}}^2 + V(\vec{r}; \{\vec{R}_i(t)\}) \right] G_\alpha(\vec{r}; \{\lambda_\alpha(t)\}) = i\hbar \frac{\partial}{\partial t} G_\alpha(\vec{r}; \{\lambda_\alpha(t)\}) \quad (II.5)$$

We use the CTA Hamiltonian in which the lattice atoms positions  $\vec{R}_i(t)$  are treated as classical fields.

To obtain equations for the time evolution of  $\lambda_\alpha(t)$  SHM expands  $V(\vec{r}; \{\vec{R}_i(t)\})$  in a power series around the instantaneous packet position  $\vec{r}_\alpha(t)$  and neglects the terms higher than second order in  $(\vec{r} - \vec{r}_\alpha(t))$ . By introducing this expansion in (II.5) and equating the coefficients of  $(\vec{r} - \vec{r}_\alpha(t))^n$ ,  $n = 0, 1, 2$  to zero SHM gives

$$\dot{\vec{r}}_\alpha(t) = \vec{p}_\alpha(t)/m \quad (II.5a)$$

$$\dot{\vec{p}}_{\alpha}(t) = -\partial V(\vec{r}_{\alpha}(t); \{\vec{R}_i(t)\}) / \partial \vec{r}_{\alpha}(t) \quad (\text{II.5b})$$

$$\begin{aligned} \dot{\overleftrightarrow{A}}_{\alpha}(t) = & -(2/m) \overleftrightarrow{A}_{\alpha}(t) \cdot \overleftrightarrow{A}_{\alpha}(t) \\ & - (1/2) \frac{\partial}{\partial \vec{r}_{\alpha}(t)} \frac{\partial}{\partial \vec{r}_{\alpha}(t)} V(\vec{r}_{\alpha}(t); \{\vec{R}_i(t)\}) \end{aligned} \quad (\text{II.5c})$$

and

$$\dot{\gamma}_{\alpha}(t) = (i\hbar/m) \text{Tr}\{\overleftrightarrow{A}_{\alpha}(t)\} + (1/2m) \vec{p}_{\alpha}(t)^2 - V(\vec{r}_{\alpha}(t); \{\vec{R}_i(t)\}). \quad (\text{II.5d})$$

Here  $\partial^2 V(\vec{r}_{\alpha}; \{\vec{R}_i\}) / \partial \vec{r}_{\alpha} \partial \vec{r}_{\alpha}$  is a matrix whose xy element is  $\partial^2 V / \partial x_{\alpha}(t) \partial y_{\alpha}(t)$ , where  $x_{\alpha}(t)$ ,  $y_{\alpha}(t)$  and  $z_{\alpha}(t)$  are the components of the vector  $\vec{r}_{\alpha}(t)$ .

These equations indicate that  $\vec{r}_{\alpha}(t)$  and  $\vec{p}_{\alpha}(t)$  follow classical trajectories with the potential  $V(\vec{r}_{\alpha}(t); \{\vec{R}_i(t)\})$ . Furthermore, one can show that the phase  $\gamma_{\alpha}(t)$  is equal to the classical action along these trajectories. The width  $\overleftrightarrow{A}_{\alpha}(t)$  has its own dynamics, with no classical analog, and depends on the force constant tensor (i.e. the second order derivatives of the classical potential).

To solve the equations (II.5) we must provide a prescription for the classical motion of the surface atoms. For this we use a method proposed by Adelman and Doll<sup>11</sup> and developed by Tully.<sup>12</sup> This provides a Langevin equation for the motion of the lattice atoms suffering the brunt of the collision.

### III. LIMITATIONS

In order to see Laue diffraction, our state must be sufficiently coherent in  $x$  and  $y$  over several unit cells to probe the surface periodicity. We accomplish this by overlapping many packets in a two dimensional grid covering a single unit cell, choosing their initial phases such that together they simulate a plane wave and using Bloch's theorem to extend this coherence over many unit cells. Following DH, this is done by making use of the identity:

$$\begin{aligned}\psi(\vec{r}, 0) &= c e^{i\vec{k}_0 \cdot \vec{r}} \\ &= c \int d\vec{r}_0 \exp\{i/\hbar[(\vec{r}-\vec{r}_0) \cdot \vec{A}_0 (\vec{r}-\vec{r}_0) + i\vec{k}_0 \cdot (\vec{r}-\vec{r}_0) \\ &\quad + i\vec{k}_0 \cdot \vec{r}_0]\} \quad (III.1)\end{aligned}$$

Replacing this integral by a sum over many equally spaced points  $\vec{r}_0^i$  produces a grid of packets which mimic a plane wave. These packets are scattered from the surface and the final state  $\psi(\vec{r}, t)$  is projected onto various outgoing plane wave states  $X(\vec{r})$ , where

$$X(\vec{r}) = \sqrt{q_z} e^{i\vec{q} \cdot \vec{r}} \quad (III.2)$$

Thus, the probability of being in a plane wave state having some wave vector  $\vec{q}$ , is the square of the  $S$  matrix

$$P(\vec{q}) = |S(\vec{q})|^2, \quad (III.3)$$

where

$$S(\vec{q}) = \langle X | \psi \rangle \quad (III.4)$$

One can show that for the case of a static lattice, it is sufficient to scatter from a single unit cell in order to calculate the diffraction probabilities.<sup>10</sup> In this paper, we also use a single unit cell, that is, we use the ADT method to propagate a four atom primary zone on the surface. The result is that we suppress the long range correlations between the motions of the surface atoms, and we therefore cannot reproduce the effect of thermal motion on the diffraction line widths. However, this does not affect the "Debye-Waller" factor for the elastic diffraction peaks, since this arises from the uncorrelated motion of individual atoms. More is said about this in Appendix 2.

Two other limitations should be mentioned: (1) the use of a single layer of packets along the z coordinate makes the incident state partially coherent. The manner in which this affects diffraction was discussed in a previous paper.<sup>13</sup> (2) the use of SHM may introduce some errors;<sup>13,14</sup> however, existing calculations agree with some exact results.<sup>10a</sup>

#### IV. Numerical results

The procedure of computation is as follows:

1. Making use of Eq. III.1, we write our initial plane wave state as a grid of packets covering the area of one unit cell. A 15 x 15 array is usually sufficient. The distance between the center of a packet and the surface is 6 Å or more.

2. Each packet is then propagated individually, is scattered from the primary zone, and its contribution to the S matrix (Eq. III.4) is computed. The initial conditions and the random fluctuations which determine the motion of the primary zone atoms are the same for each packet.

3. The S matrix contributions for all trajectories are added (coherently) and the result is squared to find the scattering probabilities.

4. The procedure is then repeated several times, using each time a different set of initial conditions and fluctuations for the lattice atoms. The results are averaged until convergence is seen. This requires only a few full runs below 100 K, and as many as 30 or more above 300 K.

Using this procedure we examine the diffraction of He and Ne from a Pt(111) surface. The atom-surface potential consists of two terms:

$$V(r) = \sum_i \left[ \frac{c_1}{|\vec{r} - \vec{R}_i|^{12}} - \frac{c_2}{|\vec{r} - \vec{R}_i|^6} \right] + \frac{c_3}{z^9} - \frac{c_4}{z^3} \quad (\text{IV.1})$$

The first is a sum of individual Lennard-Jones 6/12 interactions with several surface atoms located at  $\vec{R}_i$ . Four of these are the



primary zone atoms, and the rest (usually 10 are sufficient) surround the primary zone to help define the surface corrugation. As discussed in Tully's paper,<sup>12a</sup> the primary zone is moved along the surface so as to be always below the impinging packet. The second part of Equation (IV.1) is a bulk interaction, resulting from a pairwise summation of Lennard-Jones 6/12 interactions with all the atoms in the solid. It is only a function of  $z$ , and has the proper  $z^{-3}$  long range attractive part. The parameters  $c_1$  through  $c_4$  were chosen to produce a well depth of .125 kcal/mole and a corrugation of .19 Å for a Ne beam energy of 1.0 kcal/mole. This particular form for the potential was chosen not to mimic the actual He/Pt(111) system, which has negligible off specular scattering,<sup>15</sup> but to provide a model system with reasonable corrugation for study. The primary zone uses the parameters calculated by Tully<sup>12</sup> to simulate the actual Pt(111) surface. Unless otherwise noted, the beam energy was taken to be 1.0 kcal/mole, with an incident polar angle  $\theta = 30^\circ$  along the negative  $x$  direction ( $\phi = 0$ ).

When we calculate  $S(\vec{q})$  we generally choose  $q_x$  and  $q_y$  at or near a diffraction peak, fixing  $q_z$  by energy conservation. We could similarly choose a detector angle  $(\theta, \phi)$  and fix the magnitude of  $q$ , that is  $|\vec{q}| = |\vec{k}_0|$ , where  $|\vec{k}_0|$  is the magnitude of the initial wave vector. This is only valid in the limit of elastic scattering. If we want to describe experiments in which the energy of the scattered beam is not analysed we must integrate over all final  $|\vec{q}|$ 's, allowing for all possible final He energies. Thus the detection probability at some angle  $(\theta, \phi)$  is

$$P(\theta, \phi) = \int_0^{\infty} d|q| q^2 P(|q|, \theta, \phi) \quad (IV.2)$$

The easiest way to determine this would be to compute  $P$  at some  $(\theta, \phi)$  for several  $|q|$ 's, and add them up with the proper weighting. We again encounter a problem with beam coherence.

Our initial state has a finite width in  $z$  and covers only a single unit cell in  $x$  and  $y$ . Due to this finite spatial extent, its momentum is not so sharply defined as in a planar wave. Thus the final distribution of probabilities as a function of  $|\vec{q}|$  depends upon how much area our initial state covers. Consider Figure 1 where we plot  $P(|q|, \theta, \phi)$  for various values of  $|q|$  centered about  $|\vec{q}| = |\vec{k}_0|$  and  $(\theta, \phi)$  corresponding to the specular peak. As we increase  $N$ , where  $\psi(r, 0)$  now covers  $N \times N$  unit cells, the distribution sharpens up as expected. Thus  $P(\theta, \phi)$  in equation (IV.2) is a function of  $N$ . Since it might require very large  $N$ 's to make this dependence go away, we choose  $|\vec{q}| = |\vec{k}_0|$ . What we calculate then is the elastic DW effect, which is equivalent to doing a time of flight diffraction experiment. We confirm that it is  $N$  that dominates  $P(|q|)$  (for small  $N$ ) in Figure 2. We plot two distributions similar to figure 1 for the  $2 \times 2$  cell case, but at different temperatures. Normally the 400 K case would have a broader distribution, but both have the same  $N = 2$  limiting width.

In terms of the diffraction peak widths in real or  $k$ -space, we see the same behavior. In Figure 3 we plot  $P$  vs  $\Delta\vec{K}$  in the vicinity of the  $(1,0)$  peak.  $\Delta\vec{K}$  is the change in the parallel component of the beam momentum, in units of  $\tau$ , (the reciprocal lattice vector in the  $(1,0)$  direction). We plot  $P$  for both  $N=2$  and 3 and  $T=10K$  and 200 K. For each  $N$  we see the same peak intensities and DW effects, with only the width being different. Again the beam coherence dominates and we find their widths to be  $\tau/N$ , as in Equation A.4.

For the above He system, the  $(1,0)$ ,  $(0,1)$  and  $(1,1)$  peaks all have a reasonable probability and we consider their intensity vs. temperature in Fig. 4 where  $P(T)/P(0)$  is the ratio of the peak probability at some temperature  $T$ , to that at  $T=0$ . The curves resemble the form  $e^{-\alpha T}$  as predicted by first order

perturbation theory.<sup>2</sup> This is not surprising since He is a very light scatterer and the He/Pt mass ratio is only about .02. At higher energies and for larger atomic masses, we should see more deviation. In Fig. 5 we plot  $\ln P(T)/P(0)$  for the (1,0) and (1,1) peaks. The data resembles the straight line predicted by the Debye-Waller theories based on neutron scattering.<sup>2</sup> Note that at higher temperatures we begin to see deviations from a linear behavior. This is exactly the behavior observed experimentally, for such systems as He/Cu(100). A point to be made here concerns the two different slopes observed in Fig 5 for the (1,0) and (1,1) peak probabilities. Since these off specular peaks couple differently to the x and y components of the displacement  $\vec{U}(t)$  of the surface atom (they have a different  $\Delta k_x$  and  $\Delta k_y$ ), they show a different Debye-Waller effect. To properly predict this using the simple models would require a knowledge of the displacements, which are not equivalent for a non-cubic structure such as Pt(111).

In Fig. 6 and 7 we plot similar data for the case of Ne on Pt. The beam energy is 5.0 kcal/mole, which gives the incident Ne atoms the same velocity as the 1.0 kcal/mol He energy considered previously. Because of the larger mass ratio (0.1) we see much more energy exchange with the lattice. At 200 K the average energy change is  $-.32$  kcal/mole and  $\Delta E_{rms} = .72$  kcal/mole. For the above He system, these values were only .005 and .11 kcal/mole respectively at the same temperature. In addition to the specular we include data for the (0,2) and (-2,3) peaks, all of which show about the same intensity. Again we see a different dependence on temperature for each peak. We also see a nearly linear behavior in Fig. 7 up to about 500 K when the intensity becomes larger than a simple theory<sup>2</sup> would predict. We also see some deviations, for both He and Ne, from a linear behavior at lower temperatures, but this deviation is small.

The method proposed here seems to be able to account for the temperature dependence of diffraction peak intensities and predicts behavior similar to that observed experimentally. In order to achieve a complete description of diffraction the wave packet method should be extended to incorporate two effects: the broadening of the peak by energy and parallel momentum transfer and the resonances caused by temporary trapping at the surface (selective adsorption). As we have already discussed, the inclusion of the first effect is automatically achieved by increasing the size of the primary zone and by using enough Gaussians to cover the whole zone. This leads to a very substantial increase in the computer time. The incorporation of selective adsorption requires new theoretical developments.

#### Acknowledgements

We are grateful to Shin-Ichi Sawada, Robert Heather, Eric Heller and Gerhard Drolshagen for useful discussions. We have used a generalized Langevin program written by John Tully. One of us (HM) is very grateful to Bell Laboratories for their hospitality during an extended stay there, and in particular to John Tully for numerous and stimulating discussions. The work was supported by the National Science Foundation (NSF CHE82-06130) and in part by the Office of Naval Research.

## APPENDIX 1

We discuss here the differences between the present approach and earlier work which modified equations valid for X-ray and neutron scattering to take into account in an approximate way certain features specific to atom scattering.

The simplest way to obtain the DW factor is to examine the scattering of a projectile by the thermal average of the lattice projectile interaction. If we use a pair-wise potential  $V(\vec{r}) = \sum_{\alpha} V(\vec{r} - \vec{R}_{\alpha})$  we can write its average value as

$$\langle V(\vec{r}) \rangle = \int \frac{d\vec{k}}{(2\pi)^3} e^{-i\vec{k} \cdot \vec{r}} V(\vec{k}) \left( \sum_{\alpha} e^{i\vec{k} \cdot \vec{R}_{\alpha}^0} \right) e^{-W(\vec{k})} \quad (\text{A.1})$$

We have written here  $V(\vec{r})$  in terms of its Fourier transform  $V(\vec{k})$  and performed the average by using Bloch's formula  $\langle \exp Q \rangle = \exp[\langle Q^2 \rangle / 2]$ , where  $Q$  is any linear combination of the phonon creation and annihilation operators. The DW exponent is

$$W(\vec{k}) = (1/2) \langle (\vec{k} \cdot \delta \vec{R})^2 \rangle$$

where  $\delta \vec{R}$  is an operator representing the displacement of the lattice atom with respect to its equilibrium position (i.e. lattice site).

For X-ray and neutron scattering by the bulk of a lattice we can use perturbation theory; the transition amplitude from an initial momentum  $\vec{k}_i$  to a final momentum  $\vec{k}_f$  is then  $\langle \vec{k}_f | \langle V \rangle | \vec{k}_i \rangle$ , and this leads to a cross section proportional to

$$|V(\vec{q})|^2 \exp(-2W(\vec{q})) \left| \sum_{\alpha} \exp(i\vec{q} \cdot \vec{R}_{\alpha}) \right|^2 \delta[(\hbar^2/2m)(k_f^2 - k_i^2)], \quad (\text{A.2})$$

where  $\vec{q} \equiv \vec{k}_f - \vec{k}_i$  is the momentum transfer; the sum leads to the

Bragg conditions; the  $\delta$  function imposes energy conservation.

One can show that the DW factor  $\exp\{-2W(\vec{q})\}$  will also multiply the inelastic cross section.

Physically the DW term appears because the atoms are displaced with respect to the position of the lattice points according to a Gaussian distribution of width  $\langle \delta \vec{R}^2 \rangle$ ; the displacements of any two atoms are uncorrelated and for this reason no terms involving these displacements appear inside the sum in Eq (A.2). As a consequence, these displacements do not affect the coherence properties of the scattered beam and the diffraction line shape. Note that in its simplest form this phenomenon appears in an interference experiment in which we superimpose the interference patterns generated by a set of screens with two pinholes. In each screen the pinholes are off, by a distance  $\delta R$ , from their intended position; the probability that on a given screen the error  $\delta R$  has a specified value is given by a Gaussian; there is no correlation between the errors made for the pinholes on the same screen.

The Debye-Waller factor  $\exp\{-2W(\vec{q})\}$  appearing in Eq. (A.2) is intimately connected to perturbation theory. The general phenomenon is not. It simply has to do with the fact that the elastic scattering intensity is depressed because the thermal motion makes the atomic grating slightly faulty. The effect does not modify the line width because the errors made at different sites are uncorrelated. Thus, we can generalize the effect, as done here, by using the Langevin equation to generate the random, uncorrelated motion of the lattice atoms and not perturbative scattering theory to describe its effect on diffraction. The previous work followed a different path. It assumed that with adequate repair the neutron scattering formula (A.2) can be applied to atom scattering. (a) Since perturbation theory is not expected to work the formula was corrected in the

spirit of the distorted wave approximation. It was assumed that the atom-lattice interaction has two effects: first it speeds up the incident particle; then the accelerated particle is scattered by the hard core potential according to a formula of the type (A.2). Thus Eq. (A.2) (or its version, corrected to deal with surface rather than bulk scattering) can be used if the initial momentum appearing in it takes into account the acceleration mentioned above. This is chosen to give a kinetic energy equal to the initial kinetic energy plus the well depth. First it is not clear what permits us to divide the collision processes precisely in this way. One may argue that perhaps we should take the initial momentum zero since at the moment of impact the particle had been slowed down by the repulsive part of the potential. Furthermore the interaction with a potential of a finite range  $l$  does not create a planar wave with a large wave vector but a wave packet of width  $l^{-1}$  (in momentum). Therefore we should not use the Eq. (A.2) but a version in which the initial wave packet is a Gaussian. This would lead to different results.<sup>13</sup> Finally, on more formal grounds, we should use a  $T$  matrix rather than  $V$  and there is no clear reason why  $T(\vec{r})$  should resemble  $V(\vec{r})$  (e.g. should have a "potential well", etc.) An examination of the second order terms  $\langle V \rangle G \langle V \rangle$  in the expansion of the  $T$  matrix in terms of  $\langle V \rangle$  shows clearly that the higher order terms do not contain a DW factor of the type given by Eq. (A.2).

b) Since the pair-wise interaction between the incident atom and the solid atoms is not as well localized as the neutron-atom one, it is impossible to avoid the simultaneous interaction of the incident atom with several solid atoms; moreover successive interactions with several atoms are also important. None of these "multiple collision" events lead to a Debye-Waller like term. The attempts made to correct for such effects are not systematic<sup>2</sup> and do not seem to lead to agreement with experiment.<sup>2</sup>

## APPENDIX 2

In order to properly compute the width of a diffraction peak, using the method described in this paper, one must scatter a grid of packets from a dynamical surface of sufficient area. The width of this area is given by the correlation length  $\lambda^{-1}$ , which is the length over which the density-density correlation function for the surface atoms decays to the density squared. The nature of this decay determines the diffraction line shapes. Making the primary zone larger than  $(\lambda(T))^{-1}$  is redundant. When we scatter a beam with a cross section smaller than  $\lambda(T)^{-2}$  the beam size controls the diffraction peak width. We demonstrate this with the following simple model taken from neutron scattering.

For neutron scattering, first order perturbation theory is generally used to relate the scattering probability to the above mentioned density density correlation function. One finds,<sup>4</sup>

$$P(k') \propto \int dt e^{-i\omega t} \sum_{ij} \langle e^{+i\Delta\vec{k} \cdot \vec{R}_j(t)} e^{-i\Delta\vec{k} \cdot \vec{R}_i(0)} \rangle,$$

where  $\vec{R}_i(t)$  is the time dependent position of the  $i$ th lattice atom, and  $\Delta\vec{k} = \vec{k}' - \vec{k}$  is the change in wave vector of the scattered neutron beam. Writing this for one dimension, where  $\vec{R}_n^0 = nc$  ( $n=0,1,\dots,N$ ) labels the equilibrium position of the  $n$ th atom, we assume that the above correlation function for the fluctuations from equilibrium decays exponentially in space with some length  $\lambda^{-1}$ . Thus,

$$P(K) \propto \sum_{n,m=0}^N e^{-i\Delta k(n-m)c} e^{-\lambda|n-m|c}$$

where  $c$  is again the lattice spacing. We do the summation exactly to find



$$\begin{aligned}
P(k') \propto & \frac{N(1-e^{-2\lambda c})}{1+e^{-2\lambda c}-2e^{-\lambda c}\cos(\Delta kc)} + \frac{1-e^{-(i\Delta k+\lambda)(N+1)c}}{2-e^{-\lambda c}e^{-i\Delta kc}-e^{\lambda c}e^{i\Delta kc}} \\
& + \frac{1-e^{(i\Delta k-\lambda)(N+1)c}}{2-e^{-\lambda c}e^{i\Delta kc}-e^{\lambda c}e^{-i\Delta kc}} \quad (A.3)
\end{aligned}$$

In the limit of zero temperature,  $\lambda(t) \rightarrow 0$  (infinite correlation), and we recover the Bragg condition.

$$P(k') \propto \frac{\sin(\frac{c\Delta k(N+1)}{2})}{\sin(\frac{c\Delta k}{2})} \quad (A.4)$$

This is also the result when the beam size is smaller than  $\lambda^{-1}$ , ( $Nc < \lambda^{-1}$ ), and the surface is coherent as far as the probe can detect. In this case the peak widths are independent of  $\lambda(T)$ , having widths in  $k$ -space of  $2(Nc)^{-1}$ . As  $N$  and  $\lambda^{-1}$  become very large, we get delta function peaks.

In the opposite limit, the beam covers an area larger than the correlation length, and  $Nc > \lambda^{-1}$ . In the neighborhood of a peak, at a  $\delta k = \Delta k - 2\pi m/c$ , Eq. (A.3) reduces to

$$P(q) \propto \frac{2N}{c} \frac{\lambda}{\lambda^2 + (\delta k)^2}$$

(we assume that  $\lambda^{-1}$  is larger than a few lattice spacings). The peak structure is now independent of  $N$ , and the width is  $\lambda(T)$ , which increases with temperature. The shape of the peak is determined by the manner in which the density-density correlation function depends on distance; the Lorentzian above being a consequence of the choice of a simple exponential decay.

Thus, to generate the proper temperature dependence in the diffraction peak widths, we need to use the ADT method to propagate a primary surface larger than  $(\lambda(T))^{-1}$ , and probe it with a beam of at least this size. In general this size can be

quite large at low temperatures, requiring much computer time. However, in order to generate the proper dependence of the elastic peak intensities with temperature due to lattice motion, it is sufficient to scatter from a single unit cell. We can see this from a simple examination of the neutron scattering cross section for a thermal lattice. This expression can be written in terms of the density-density correlation function for the lattice atoms mentioned earlier. That is

$$P \propto \int_{-\infty}^{\infty} dt \, e^{-i\omega t} \int d\vec{r} \, e^{i\Delta\vec{k} \cdot \vec{r}} G(\vec{r}, t)$$

where

$$G(\vec{r}, t) = \frac{1}{N} \int d\vec{r}' \langle \rho(\vec{r}' - \vec{r}, 0) \rho(\vec{r}', t) \rangle .$$

It is possible to divide this expression into a sum of elastic (time independent) and inelastic (time dependent) terms by taking

$$G(\vec{r}, t) = G(\vec{r}, \infty) + G'(\vec{r}, t)$$

where  $G(\vec{r}, \infty)$  is time independent since

$$\lim_{t \rightarrow \infty} \langle \rho(\vec{r}, t) \rho(0, 0) \rangle = \langle \rho \rangle^2 .$$

The elastic peak intensity is thus

$$P_{el} \propto \left| \int d\vec{r} \, e^{i\Delta\vec{k} \cdot \vec{r}} \langle \rho(\vec{r}) \rangle \right|^2 \propto \sum_{\vec{\tau}} \delta(\Delta\vec{k} - \vec{\tau}) \exp[-2W(\vec{\tau})]$$

where  $\vec{\tau}$  are the reciprocal lattice vectors of the solid. The Debye-Waller factor  $\exp[-2W(\vec{\tau})]$ , therefore, is related to the Fourier transform of the density operator for a single lattice site. All site to site time and spatial correlations lead to energy and momentum transfer (i.e., inelastic processes), and are included in  $G'(\vec{r}, t)$ .

## REFERENCES

1. For recent reviews see:
  - a) V. Celli, "Elastic and Inelastic Atom-Surface Scattering, in Many-Body Phenomena at Surfaces" (Academic Press, NY, 1984), D. Langreth and H. Suhl, eds; b) T. Engel and K.H. Rieder, "Structural Studies of Surfaces with Atomic and Molecular Beam Diffraction", Structural Studies of Surfaces (Springer-Verlag, N.Y., 1982); c) M.J. Cardillo, Ann. Rev. Phys. Chem., 32, 331, 1981; d) H. Hoinkes, Rev. Mod. Phys., 52, 933, 1980; e) M.W. Cole and D.R. Frankl, Surf. Sci., 70, 585, 1978; f) H. Wilsch, "Topics in Surface chemistry", eds. E. Kay and P. Bagus, Plenum Press, N.Y., 1978, p. 135; g) F.O. Goodman, CRC Crit. Rev. in Solid State and Mat. Sci., 7, 33, 1977; and h) F.O. Goodman and H.Y. Wachman, "Dynamics of Gas-Surface Scattering," Academic Press, NY, 1976.
2.
  - a) G. Comsa, J. Phys., C Solid State Phys., 6, 2648, 1973; b) J.L. Beeby, J. Phys C, Solid State Phys., 4, L359, 1971, 5, 3438, 1972, 5, 3457, 1972, 6, 1229, 1973; c) J. Lapujoulade, Y. Lejay, and G. Armand, Surf. Sci., 95, 107, 1980; d) A.C. Levi and H. Suhl, Surf. Sci., 88, 221, 1979; e) H. Frank, H. Hoinkes, and H. Wilsch, Surf. Sci., 63, 121, 1977; f) W.H. Weinberg, J. Chem. Phys., 57, 5463 (1972).
3. H. Hoinkes, H. Nahr, and H. Wilsch, Surf. Sci., 33, 516, 1972, 40, 457, 1973, and 30, 363, 1972.
4. W.M. Marshall and S.W. Lovesey, Theory of Thermal Neutron Scattering, Oxford, Clarendon Press, 1971.
5. A.A. Maradudin, E.r. Montroll, G.H. Weiss, and I.P. Ipatova, "Theory of Lattice Dynamics in the Harmonic

Approximation", Academic Press, NY, 1971, p. 326.

6. a) For an overview see Reference 1 (b); b) R.B. Laughlin, Phys. Rev. B25, 2222, 1982; c) A. Liebsh, J. Harris, B. Salanon, and J. Lapujoulade, Surf. Sci., 123, 338, 1982; d) G. Drolshagen, A. Kaufhold, J.P. Toennies, Isr. J. Chem., 22, 283, 1982; e) K.H. Rieder, N. Garcia, V. Celli, Surf. Sci., 108, 169, 1981; f) G. Armand, J. Lapujoulade, J.R. Manson, Surf. Sci., 82, L625, 1979; G. Armand, J.R. Manson, Phys. Rev., 13, 18, 6510, 1978, Phys. Rev. Lett., 43, 1839, 1979, Surf. Sci., 80, 532, 1979; h) N. Garcia and N. Cabrera, Phys. Rev. B18, 576, 1978; i) F.O. Goodman, J. Chem. Phys., 66, 976, 1977; j) C.J. Ray and J.M. Bowman, J. Chem. Phys., 66, 1122, 1977; 63, 5231, 1975; k) R.I. Masel, R.P. Merrill, and W.H. Miller, Phys. Rev. B12, 5345, 1975, J. Chem. Phys. 65, 2690, 1976.
7. A. Messiah, Quantum Mechanics, Vol 2, (Northa Holland, Amsterdam).
8. a) H. Metiu and G. Schon, Phys. Rev. Lett., 53, 13, 1984; b) S.D. Augustin and H. Rabitz, J. Chem. Phys., 69, 4195 (1978).
9. a) E.J. Heller, J. Chem. Phys., 62, 1544 (1975); b) *ibid.*, 65, 4979 (1976); c) K.C. Kulander and E.J. Heller, *ibid.*, 69, 2439 (1978); d) E.J. Heller, *ibid.*, 68, 2066, 3891 (1978); e) S.Y. Lee and E.J. Heller, *ibid.*, 71, 4777 (1978); f) M.J. David and E.J. Heller, *ibid.*, 71, 3383 (1979); g) R.B. Brown and E.J. Heller, *ibid.*, 75, 186 (1981); h) S.Y. Lee and E.J. Heller, *ibid.*, 76, 3035 (1982); i) D.J. Tannor and E.J. Heller, *ibid.*, 77, 202 (1982); j) E.J. Heller, R.L. Sundberg, and D. Tannor, *ibid.*, 86, 1822 (1982); k) N. DeLeon and E.J. Heller, *ibid.*, 78, 4005 (1983).

10. a) G. Drolshagen and E. Heller, J. Chem. Phys., 79, 2072 (1983); b) G. Drolshagen and E. Heller, Surface Sci., 139, 260 (1984).
11. a) S.A. Adelman and J.D. Doll, J. Chem. Phys., 64, 2375 (1976); b) S.A. Adelman, J. Chem. Phys., 71, 4471 (1979); c) S.A. Adelman and B.J. Garrison, J. Chem. Phys., 65, 3751 (1976); d) J.D. Doll and D.R. Dion, J. Chem. Phys., 65, 3762 (1976); (e) S.A. Adelman Adv. Chem. Phys., 44, 143 (1980); J. Doll, in Aerosol Microphysics, ed. W.H. Marlow (Springer, New York, 1980).
12. a) J.C. Tully, J. Chem. Phys., 73, 1975 (1980); b) M. Shugard, J.C. Tully and A. Nitzan, J. Chem. Phys., 66, 2534 (1977); (b) J.C. Tully, Annu. Rev. Phys. Chem., 31, 319 (1980).
13. B. Jackson and H. Metiu, J. Chem. Phys. (in press).
14. A detailed numerical and theoretical analysis of the strategy of packet propagation was carried out by S. Sawada, R. Heather, B. Jackson and H. Metiu and it is being prepared for publication.
15. J. Lee, J.P. Cowin and L. Wharton, Surface Sci., 130, 1 (1983).

### Figure Captions

- Figure 1. Velocity distribution of scattered beam relative to average initial velocity ( $\hbar k_0/m$ ) for an initial grid of packets covering  $N \times N$  cells, where  $N=1$  (XXXXX), 2(-.-.-.-.), 3(-----), and 4(———). Surface temperature is 100 K.
- Figure 2. Same as above for  $N=2$  case, except the surface temperatures are 100 K (XXXXX) and 400 K (000).
- Figure 3. Peak probability vs.  $\Delta K$ .  $\Delta K$  is in units of the reciprocal lattice vector in the (1,0) direction (i.e.,  $\Delta K = 1.0$  marks the (1,0) peak). The plots are for an initial grid covering  $N \times N$  unit cells, where  $N=2$ ,  $T=10K$  (———),  $N=2$ ,  $T=200K$  (-----),  $N=3$ ,  $T=10K$  (0000), and  $N=3$ ,  $T=200K$  (-0-0-0-0). Note that peak height is independent of  $N$ , which only affects the width.
- Figure 4. Peak probabilities  $P(T)$  as a function of surface temperature, relative to static lattice values  $P(0)$ , for the (1,0) ( $\diamond\diamond\diamond$ ), (2,0) (000), and (1,1)(XXXX) peaks for He/Pt(111).
- Figure 5. Log of the relative probabilities of Fig. 4 vs. temperature, for the (1,0) (0000) and (1,1) ( $\diamond\diamond\diamond$ ) peaks.
- Figure 6. Peak probability vs. temperature for the (0,0) ( $\diamond\diamond\diamond$ ) (2,0) (0000), and (-2,3)(XXXX) peaks of Ne/Pt(111).
- Figure 7. Log of the probabilities in Fig. 6 vs. temperature for the (0,0) (0000) and (2,0) ( $\diamond\diamond\diamond$ ) peaks.

fig. 1

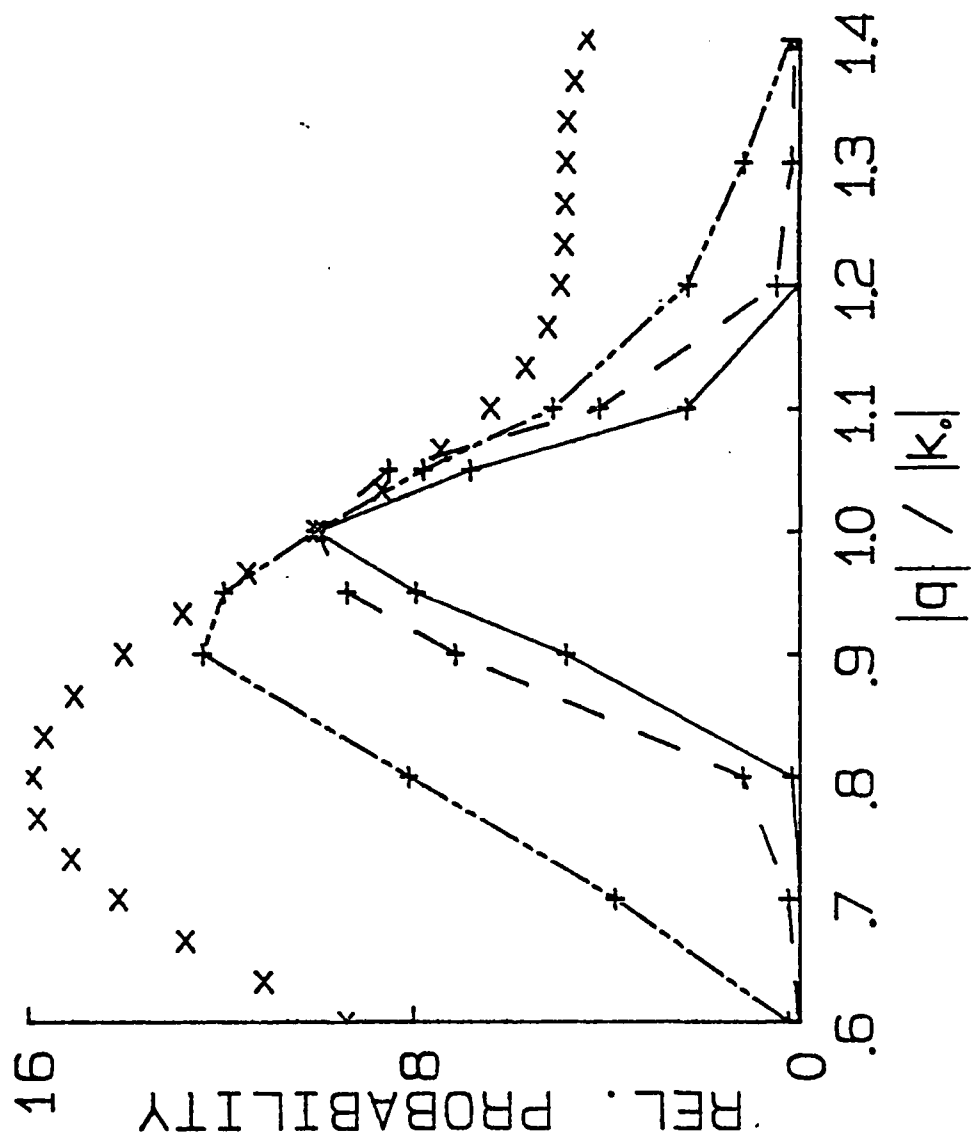


fig. 2

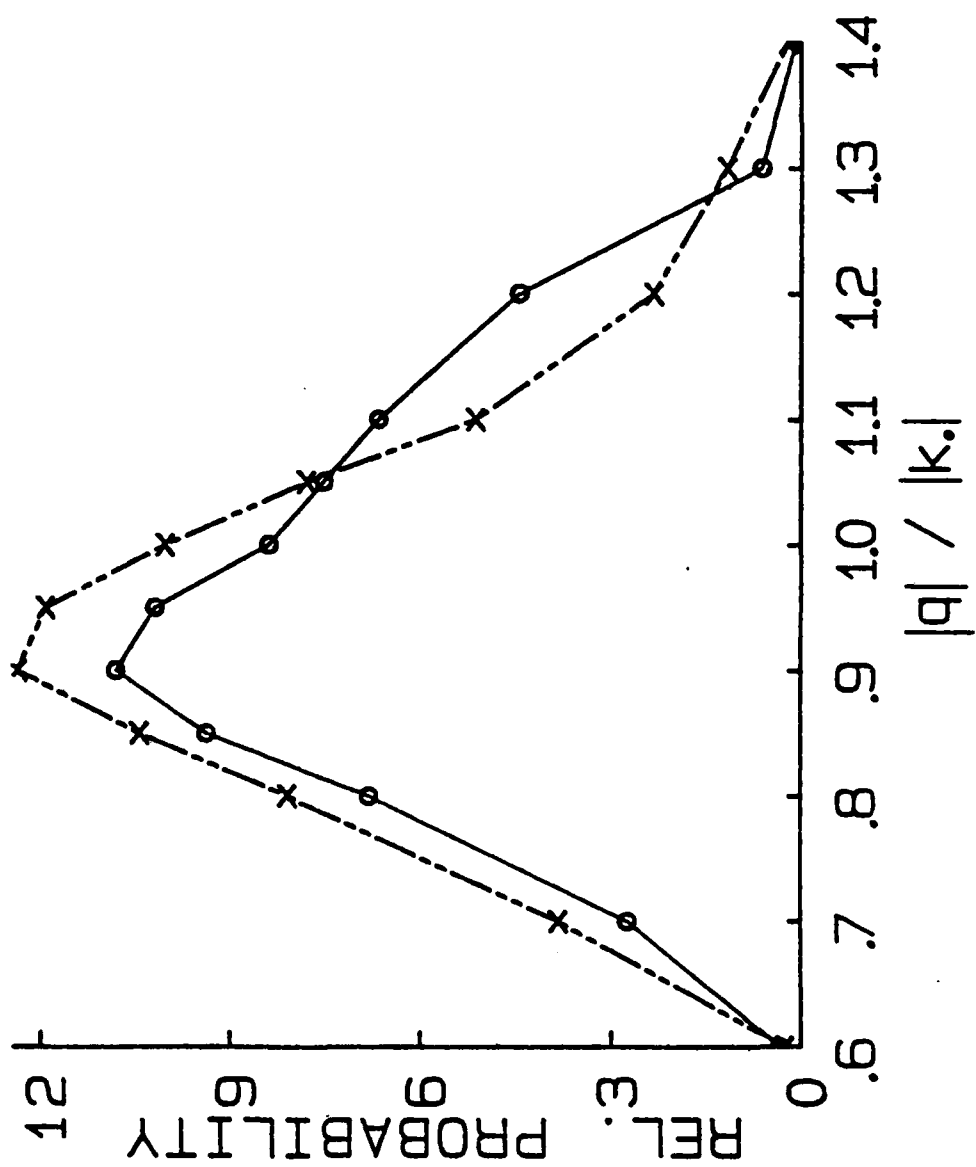




Fig. 3.

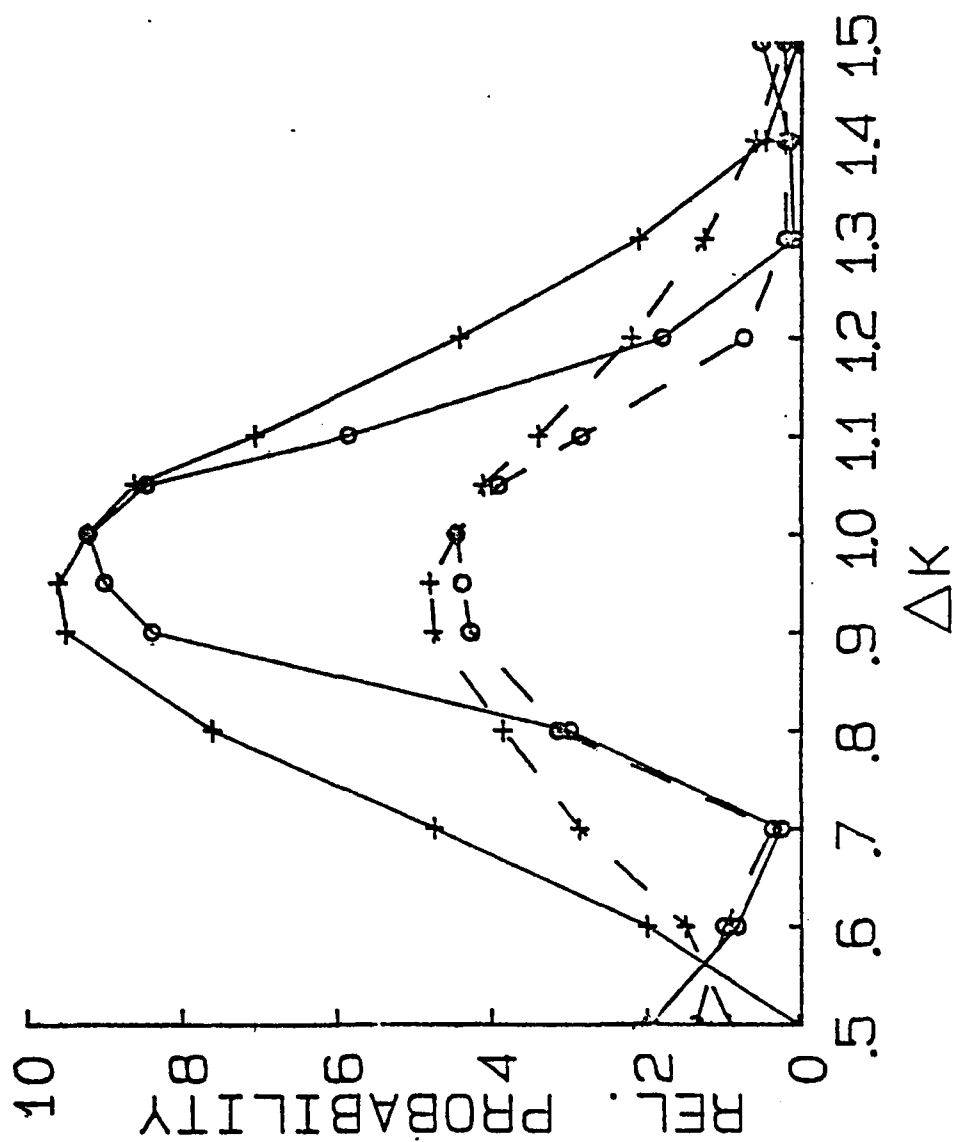


fig. 4

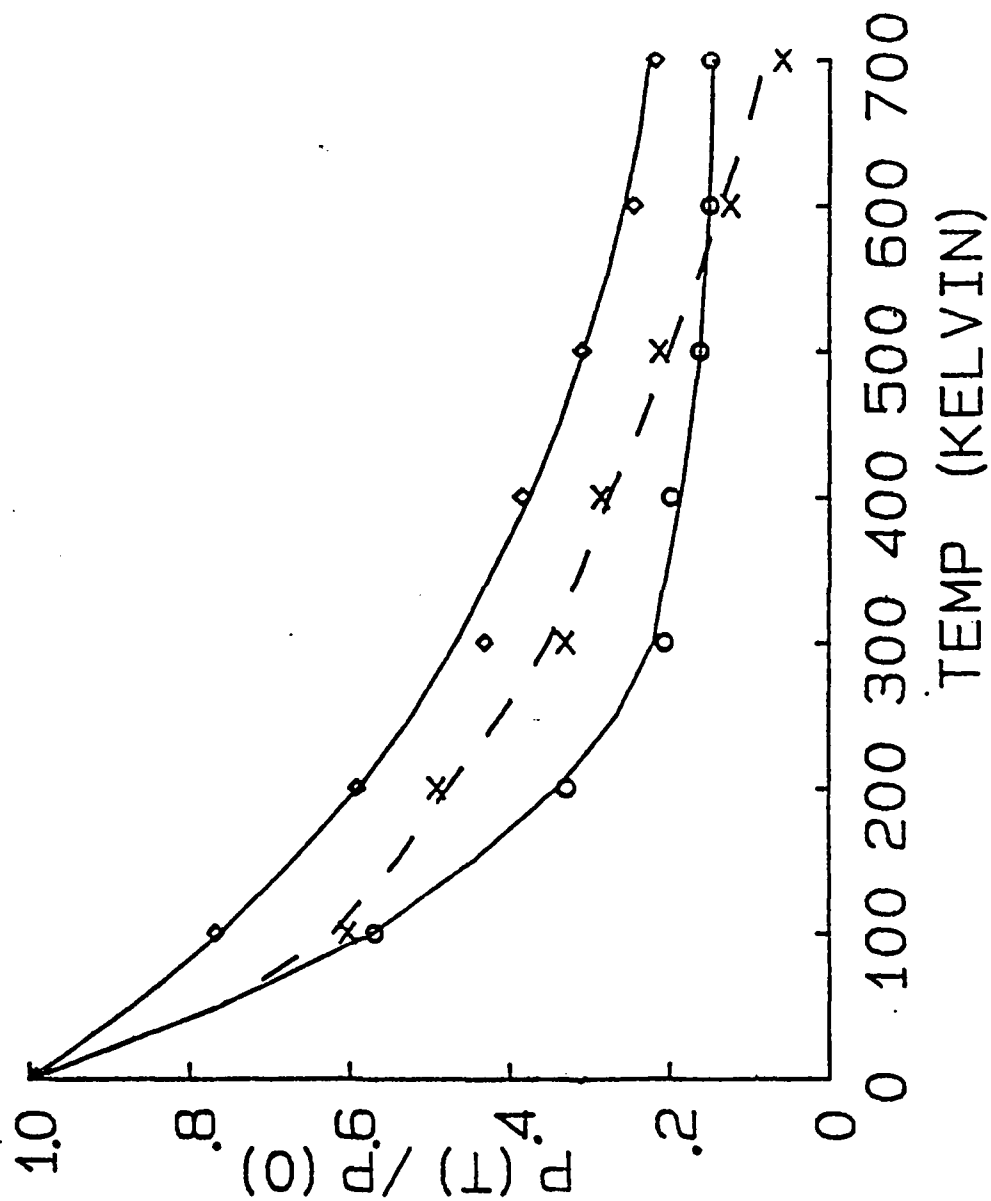


fig. 5

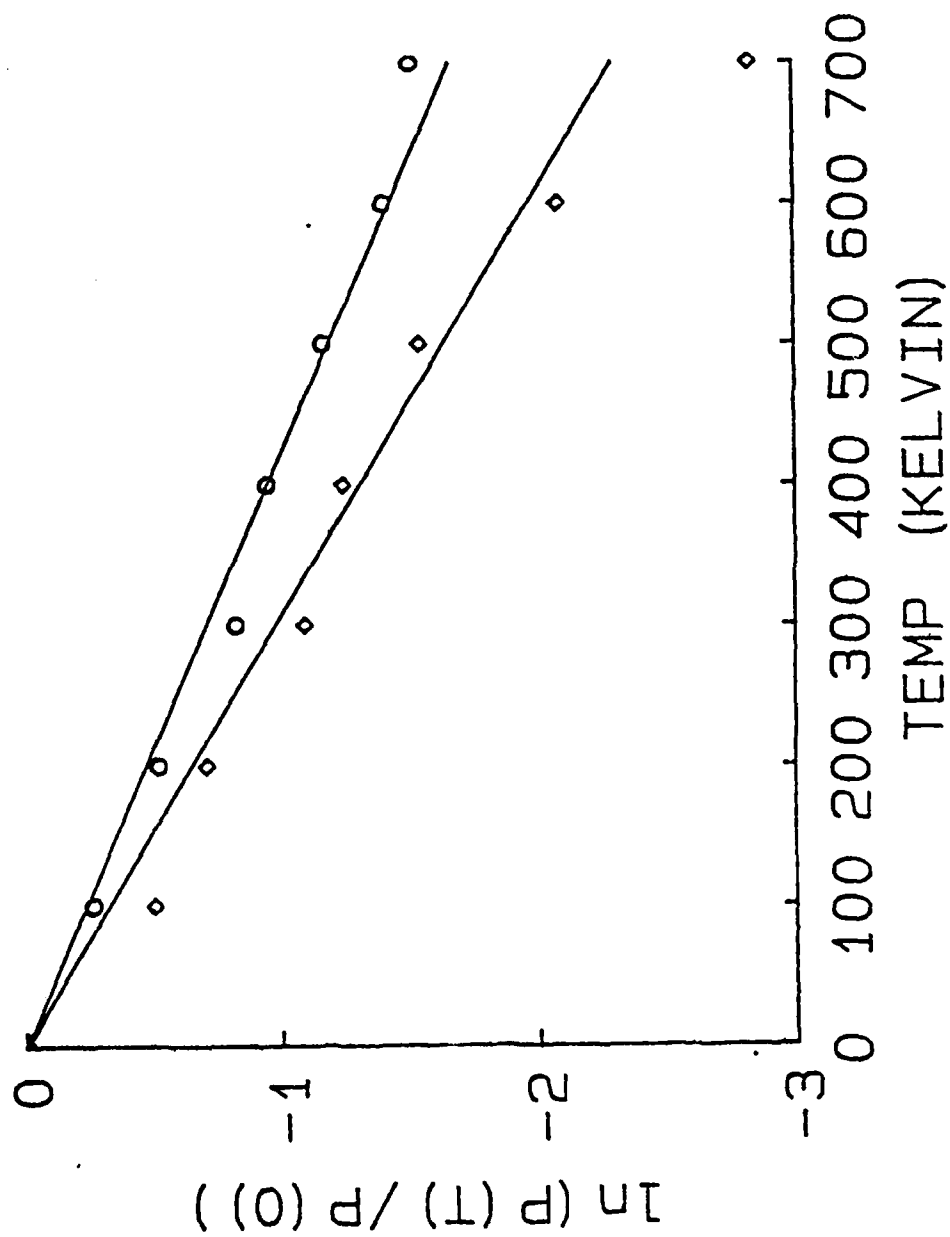


fig. 6

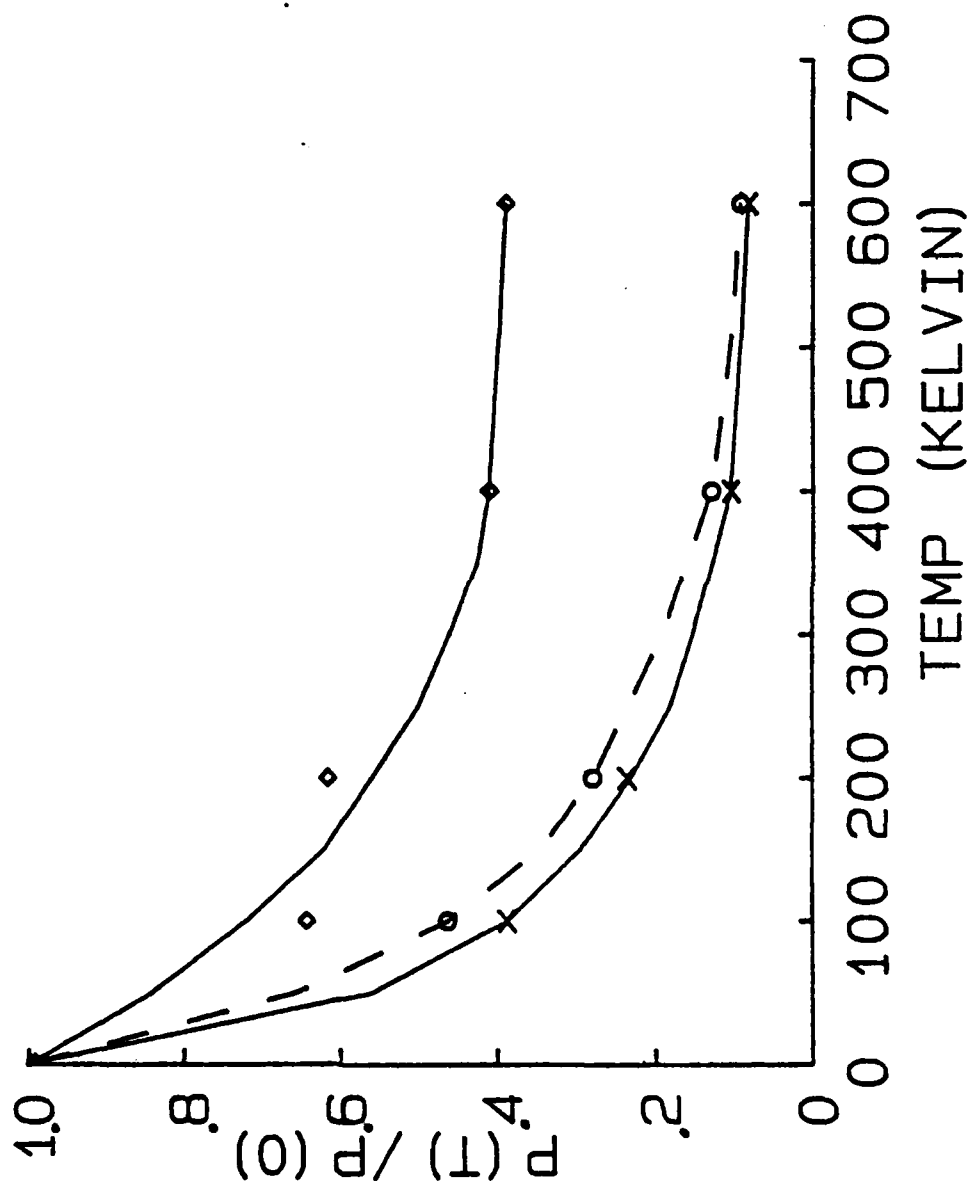
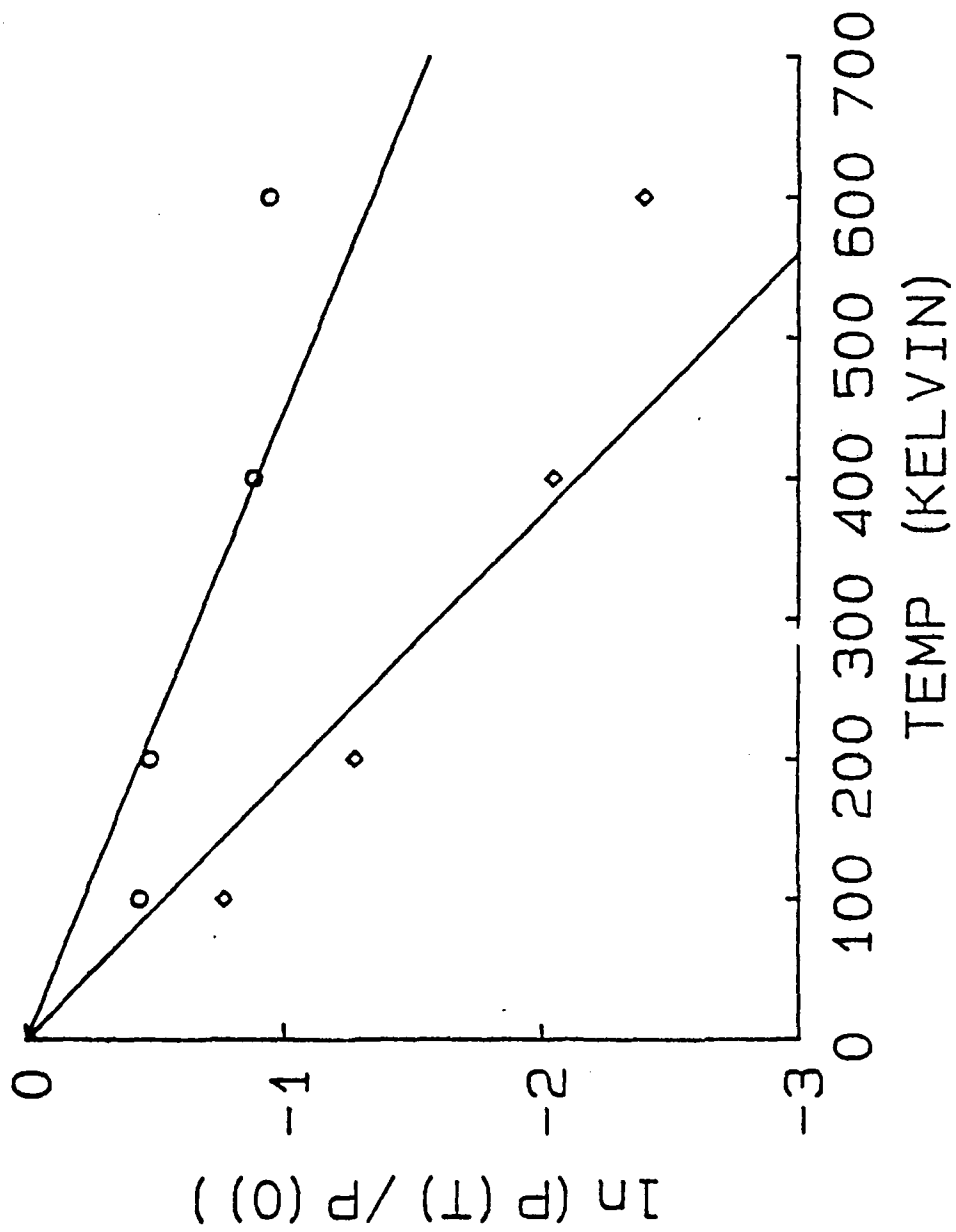


fig. 7



**END**

**FILMED**

**5-85**

**DTIC**